

AD-A055 443

PRATT AND WHITNEY AIRCRAFT GROUP WEST PALM BEACH FL 6--ETC F/G 11/6  
TITANIUM ALLOY IGNITION AND COMBUSTION.(U)

JAN 78 V G ANDERSON, B A MANTY

UNCLASSIFIED

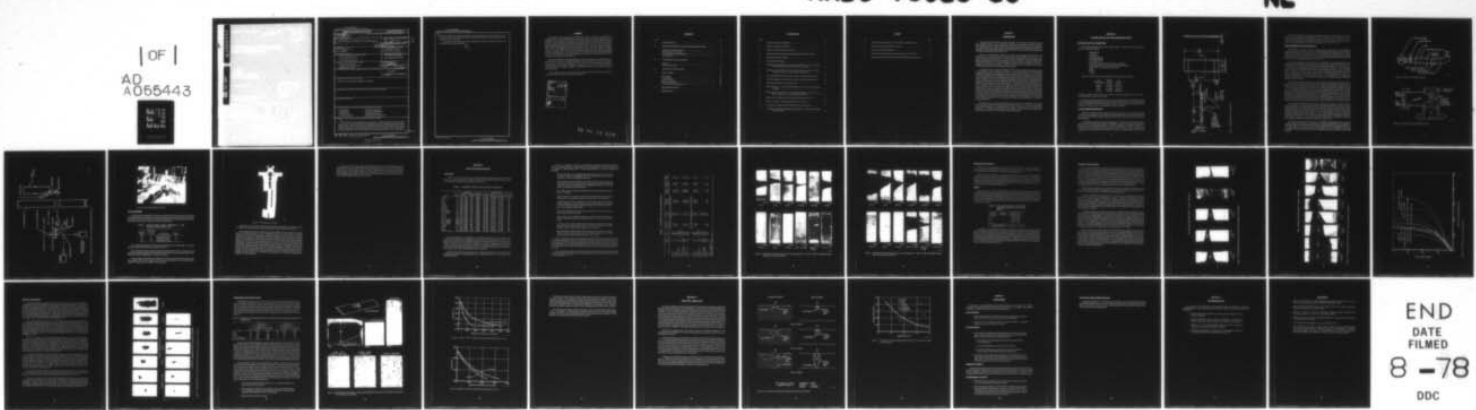
PWA-FR-9511

NADC-76083-30

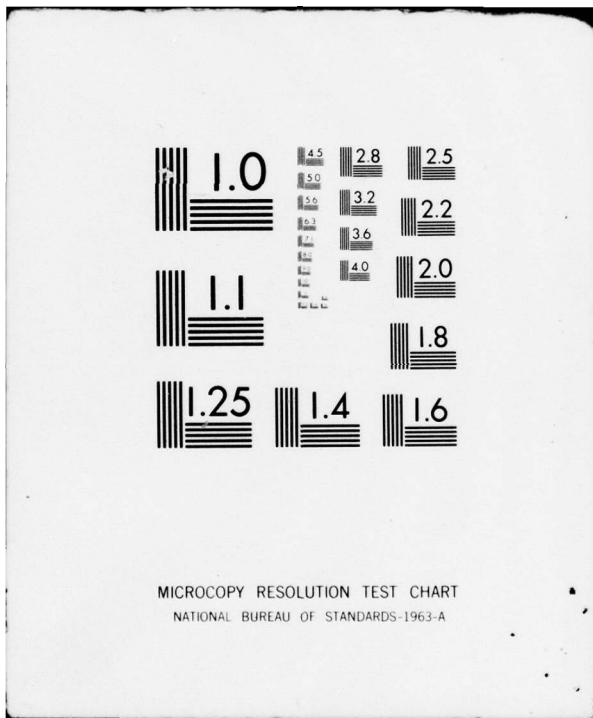
N62269-76-C-0429

NL

| OF |  
AD  
A056443  
REF ID:  
A056443



END  
DATE  
FILMED  
8 -78  
DDC



MICROCOPY RESOLUTION TEST CHART  
NATIONAL BUREAU OF STANDARDS-1963-A

DOC FILE COPY

ADA055443

UNCLASSIFIED

SECURITY CLASSIFICATION OF THIS PAGE (When Data Entered)

**DD FORM 1 JAN 73 1473 EDITION OF 1 NOV 65 IS OBSOLETE**  
**S/N 0102-LF-014-6601**

UNCLASSIFIED

SECURITY CLASSIFICATION OF THIS PAGE (When Data Entered)

**UNCLASSIFIED**

**SECURITY CLASSIFICATION OF THIS PAGE (When Data Entered)**

chromium-molybdenum coating significantly reduced the magnitude of burn and an ion vapor deposited aluminum coating prevented ignition. The higher temperature environment was shown to produce a more severe burn.

Comparison of one test run with results predicted by the analytical model currently under development showed good agreement.

S/N 0102- LF- 014- 6601

**UNCLASSIFIED**

**SECURITY CLASSIFICATION OF THIS PAGE(When Data Entered)**

## SUMMARY

The objective of this program was to delineate the relative ignition and combustibility of titanium alloys and the environmental areas where fires could occur. Nine titanium alloys were included in this evaluation. In addition, two of these alloys, Ti 6Al-2Sn-4Zr-2Mo and Ti 8Al-1Mo-1V, were coated with chromium-molybdenum to determine its effectiveness in reducing ignition and sustained combustion. A specimen of Ti 8Al-1Mo-1V was also coated with ion vapor deposited (IVD) aluminum. Each alloy was subjected to test at two environmental conditions: 240°C (400°F)—0.62 MPa (90 psia)—122 m/sec (400 ft/sec), and 427°C (800°F)—0.48 MPa (70 psia)—213 m/sec (700 ft/sec). In a test rig capable of establishing these conditions each alloy specimen was subjected to a CO<sub>2</sub> laser beam as an ignition source. A high-speed photographic record was made of each test run which permitted a one frame per millisecond resolution of the specimen burn propagation characteristics.

Results indicated that only slight differences could be found in the burn characteristics of Ti 8Al-1Mo-1V, Ti 6Al-4V, Ti 6Al-2Sn-4Zr-2Mo, Ti 6Al-2Sn-4Zr-6Mo, Ti 6Al-6V-2Sn and Ti 8Mn alloys. Ti 13V-11Cr-3Al, Ti<sub>3</sub>Al and Ti 13Cu did not burn. The chromium-molybdenum coating significantly reduced the degree of specimen burn and the IVD aluminum coating prevented ignition. The higher temperature environmental condition was shown to produce a more severe burn.

The comparison of one test run with results predicted by the analytical model, currently under development by P&WA, showed good agreement.

ACCESSION for	
NTIS	White Section <input checked="" type="checkbox"/>
DDC	Buff Section <input type="checkbox"/>
UNANNOUNCED	<input type="checkbox"/>
JUSTIFICATION	<input type="checkbox"/>
BY	
DISTRIBUTION/AVAILABILITY CODES	
Dist.	AVAIL. and/or SPECIAL
A	

78 06 15 050  
ii

## CONTENTS

<i>Section</i>		<i>Page</i>
I	INTRODUCTION.....	1
II	TITANIUM IGNITION AND FIRE PROPAGATION TESTS.....	2
	Materials and Test Conditions.....	2
	Test Specimen Preparation.....	2
	Test Equipment and Configuration.....	4
	Test Procedure.....	7
III	TEST RESULTS AND ANALYSIS.....	10
	Test Data.....	10
	Analysis of Test Data.....	15
IV	ANALYTICAL SIMULATION.....	26
V	CONCLUSIONS.....	29
	Alloy Effects.....	29
	Coating Effect.....	29
	Geometry Effects.....	29
	Environmental Effects.....	29
	Analytical Model Substantiation.....	30
VI	RECOMMENDATIONS.....	31
	REFERENCES.....	32

## ILLUSTRATIONS

<i>Figure</i>		<i>Page</i>
1	Titanium Specimen Configuration.....	3
2	Titanium Combustion Test Rig.....	5
3	Titanium Combustion Rig Test Section.....	5
4	Arrangement of Laser Ignition and Photographic Recording Systems.....	6
5	Laser Airfoil Ignition Test Rig.....	7
6	Test Specimen in Holder.....	8
7	Appearance of Test Specimens After Laser Impingement in 240°C (400°F), 0.62 MPa (90 psia), 122 m/sec (400 ft/sec) Airstream.....	13
8	Appearance of Test Specimens After Laser Impingement in 427°C (800°F), 0.48 MPa (70 psia), 213 m/sec (700 ft/sec) Airstream.....	14
9	Test Alloys Ranked by Burn Severity (Percent of Exposed Area Burned)....	17
10	Test Alloys Ranked by Burn Severity (Percent of Exposed Area Burned)....	18
11	Time-Distance Travel of Combustion Front.....	19
12	Burn Propagation of Coated and Uncoated Ti 6-2-4-2 at Low Temperature Condition.....	21
13	Metallographic Examination of Chromium-Molybdenum Coated Ti 6-2-4-2 After Testing Under Low Temperature Conditions.....	23
14	Effect of Test Conditions On Temperature Distribution in Ti 8-1-1.....	24
15	Effect of Coating on Temperature Distribution in Ti 8-1-1.....	24
16	Comparison of Analytical Simulation With Actual Test Results.....	27
17	Comparison of Flowwise Burning Rate for Run No. 2-1 Predicted by Model and as Measured.....	28

## **TABLES**

<i>Table</i>		<i>Page</i>
1	Laser Power Losses Observed in the Titanium Combustion Test.....	7
2	Specimen Initial Data and Run Conditions.....	10
3	Specimen Test Data and Results.....	12
4	The Relationship Between Specimen Thickness and Laser Effect.....	15
5	Depths of Microstructural Changes From Metallographic Examination.....	22

## **SECTION I**

### **INTRODUCTION**

Titanium and titanium alloys are used extensively in aerospace systems because of their high strength-to-density ratio, temperature resistance and excellent corrosion behavior. Titanium alloys have been widely applied to aircraft structural components and to turbine engine and compressor parts. As titanium alloys have found application in different environments, especially at increasingly higher temperatures and pressures, a renewed interest has developed in their ignition and combustion behavior in air.

Ignition and self-sustained combustion are closely related phenomena but differ in one important aspect, the primary source of thermal energy being supplied to the system. In the ignition process, energy is supplied to the system from a combination of metal oxidation plus energy from external sources, such as radiation, mechanical friction or aerodynamic heating. In self-sustained combustion, the energy supplied by metal oxidation is sufficient, without any additional input from other sources, to balance heat loss due to all modes of heat transfer, including heat absorbed in thermodynamic phase change.

An in-depth study was initiated at P&WA in 1973 to develop the analytical methods needed to quantitatively evaluate titanium combustion in gas turbine engines. The study, which included both analytical and experimental efforts, resulted in the development of an analytical model for the prediction of self-sustained combustion of titanium airfoils. The model, based on a thermal balance between heat generated in the combustion process and that lost by all modes of heat transfer, was found to yield reasonable agreement with the results of the experimental program for burning near the lower combustion limit. This model, which was formulated for two-dimensional thermal flow, has been generalized for three-dimensional flow and programmed for computer solution. Modifications were also made to the details of the thermal convection model in the combustion zone to provide better agreement with test results at high burning rates. P&WA is now conducting a separate program under Contract F33615-76-C-5041, to develop and substantiate an analytical method for the prediction of ignition and self-sustained combustion of titanium. In the course of this program, the titanium combustion model will be further tested for its general validity, and improved, as necessary, so that the resulting analytical system provides a tool which will not only predict the occurrence of ignition and fire propagation in titanium gas turbine engine components, but will also allow the design of such components to prevent or minimize such fires.

The objective of the program described in this report was to delineate the relative combustibility of titanium alloys and the areas where fires could occur. This work complemented the model development by substantiating its ability to predict ignition and propagation phenomenon of several titanium alloys while providing combustion data comparing the performance of titanium alloys commonly used in naval aircraft.

## SECTION II

### TITANIUM IGNITION AND FIRE PROPAGATION TESTS

#### MATERIALS AND TEST CONDITIONS

The following titanium alloys were evaluated relative to ignition and burn propagation properties during this program:

Ti 8Al-1Mo-1V  
Ti 6Al-4V  
Ti 6Al-6V-2Sn  
Ti 6Al-2Sn-4Zr-2Mo  
Ti 6Al-2Sn-4Zr-6Mo  
Ti 13V-11Cr-3Al  
Ti 8Al-1Mo-1V coated with chromium-molybdenum  
Ti 6Al-2Sn-4Zr-2Mo coated with chromium-molybdenum  
Ti 8Al-1Mo-1V coated with IVD aluminum  
Ti<sub>3</sub>Al  
Ti 8Mn  
Ti 13Cu

These alloys were evaluated at the following two environmental conditions:

Air Temperature	Chamber Pressure	Air Velocity
427°C (800°F)	0.48 MPa (70 psia)	213 m/sec (700 ft/sec)
240°C (400°F)	0.62 MPa (90 psia)	122m/sec (400 ft/sec)

In addition a single specimen of Ti 13Cu-1.5Al was run at test conditions of 427°C (800°F)—0.62 MPa (90psia)—213 m/sec (700 ft/sec).

The above conditions correspond to test run environments previously established as being capable of permitting ignition and sustained combustion of Ti 8Al-1Mo-1V. The selection of these specific environmental conditions was based on their close proximity to the lower limit of sustained combustion to favor the identification of alloy differences.

#### TEST SPECIMEN PREPARATION

Airfoil test specimens were prepared from the above alloys by tracer machining and polishing to the configuration shown on Figure 1. Machining difficulty with certain alloys resulted in some variation in both specimen thickness and width. This variation was most severe in the Ti 8Mn specimens.

The appropriate samples were then vapor blasted to a uniform matte finish and provided with the required coatings. The chromium-molybdenum coatings were applied, as described in Reference 1, to the established thickness of 0.0127 mm (0.0005 in.) to 0.0381 mm (0.0015 in.). Coating of the Ti 8-1-1 alloy with ion vapor deposited (IVD) aluminum, type II - chromated, was performed by the McDonnell Aircraft Company to a thickness of approximately 0.025 mm (0.001 in.).

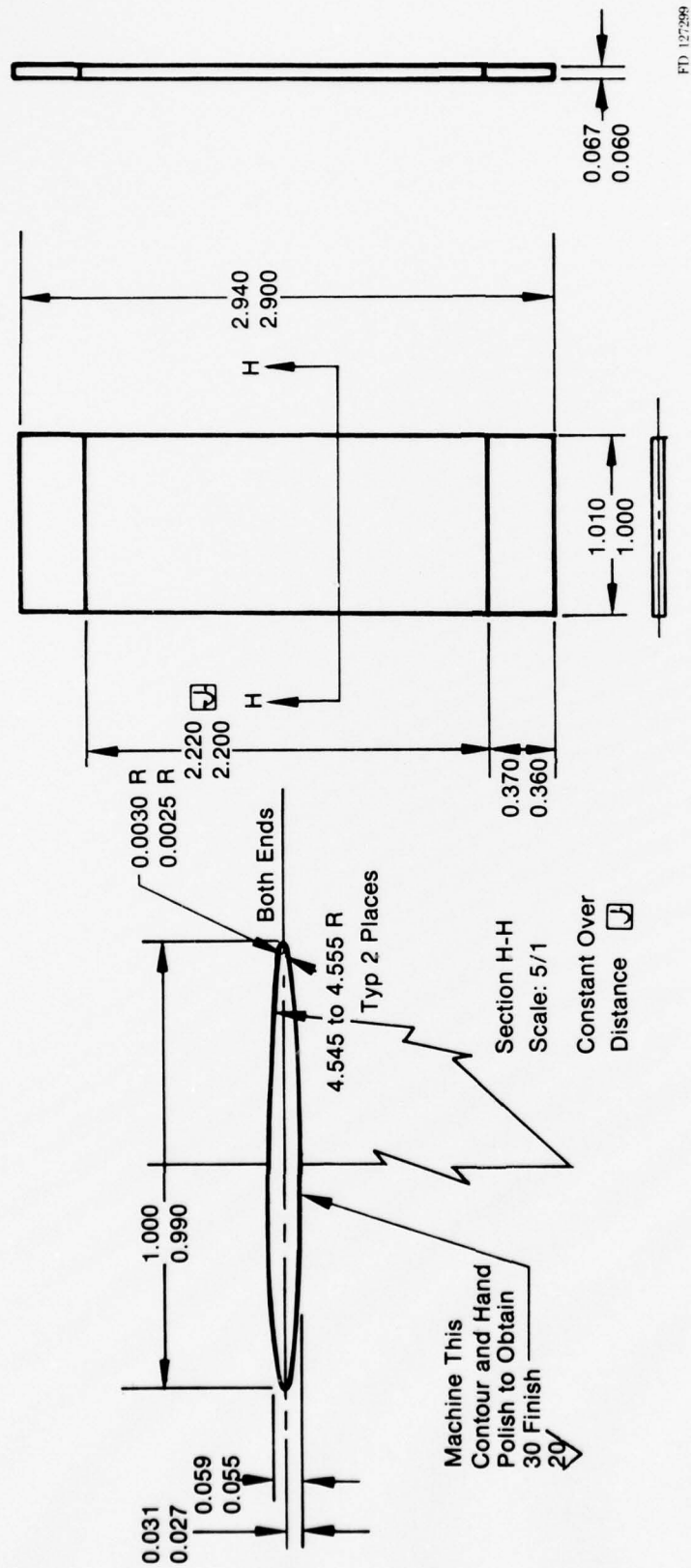


*Figure 1.* Titanium Specimen Configuration

In a final preparation step, each specimen was coated with black nickel in the area of planned laser impingement in accordance with the procedure provided in Reference 2. This coating serves to equalize the coupling of laser energy to the specimen by eliminating variations caused by reflectivity differences among the various alloys. After preparation was complete, each specimen was weighed and an "eyelash" profile made of the airfoil cross section.

### TEST EQUIPMENT AND CONFIGURATION

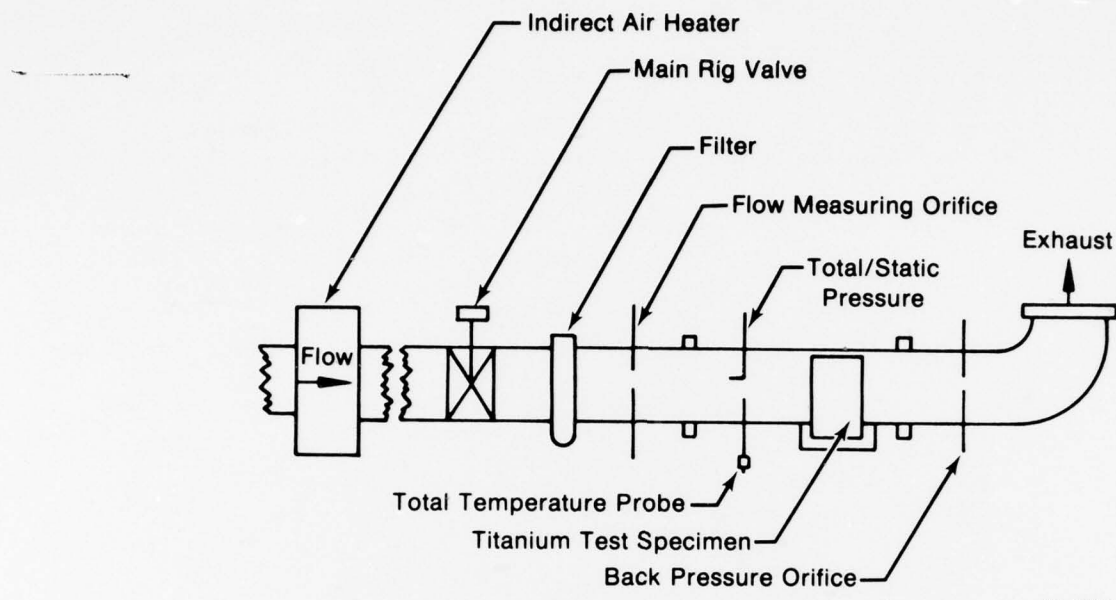
The P&WA test facility is a small compressor-driven wind tunnel, with appropriate conditioning equipment, to allow simulation of a wide range of environmental conditions. Facility capabilities encompass air pressure (up to 0.97 MPa (140 psia)), temperature (up to 538°C (1000°F)) and velocity (up to 335 m/sec (1100 ft/sec)). Small airfoil test specimens are mounted in a rectangular two-dimensional test section. Appropriate instrumentation is provided to measure airflow, total and static pressure and total temperature.

The overall arrangement of the test rig is shown in Figure 2. Air is supplied from a large compressor, passed through a gas-fired indirect air heater and is metered and filtered prior to entering the test section. The test section shown schematically in Figure 3, is a 1.91 cm (0.75 in.) by 5.08 cm (2.0 in.) rectangular channel with a bellmouth inlet and 7.62 cm (3.0 in.) of straight section upstream of the airfoil leading edge. The test specimen mounts in a cylindrical carrier which is inserted into the test section. Orifice plates, upstream and downstream of the test section, provide control of the flowrate and pressure level. Thermocouples are positioned to provide temperatures at the flow-measuring orifice, in the specimen test chamber and downstream of the specimen. Airstream flow is determined by calculation using the differential pressure across the orifice.

The test section is provided with two optical windows for irradiation and viewing of the test specimens. These windows are mounted in a port on the side of the rig and are located 20.3 cm (8.0 in) from the test specimen. The window for the camera is fused quartz, optically flat, which is 6.35 cm (2.5 in.) in diameter and 1.27 cm (0.5 in.) thick. The laser beam window is 3.81 cm (1.5 in.) in diameter and 0.64 cm (0.25 in.) thick zinc selenide. This material offers excellent transmissivity for the 10.6 micron wave-length emission of the CO<sub>2</sub> laser beam. The zinc selenide window has an antireflective coating on both faces to minimize reflection and scatter of the beam. The quartz window has excellent optical clarity for visible light but it will not transmit the CO<sub>2</sub> laser light, thus protecting the camera lens from scattered reflections of the laser beam. The windows are protected from the high-temperature test environment by a water jacket to absorb conducted heat in the metal housing and an air injection system to film cool the optical surfaces.

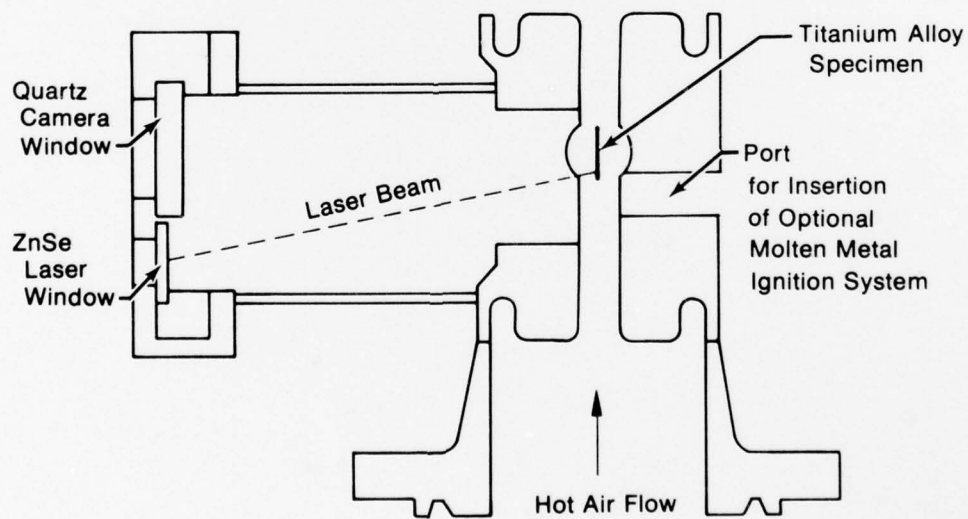
The arrangement of the test section and other supporting test equipment is shown in Figures 4 and 5. Because of environmental requirements, the laser equipment is located in the air conditioned control room and the beam passed through a port in the concrete blast wall. A high-speed Fairchild motion picture camera and a video camera with tape recording system with tape playback capability are arranged, through the use of a beam splitter, to permit simultaneous photographic and real time video observation. The energy required for specimen ignition is supplied by a CRL Model 41 laser. This laser system is an electric discharge, water cooled CO<sub>2</sub> laser capable of providing an output of approximately 250 watts in the TEM 00 (Transverse Electromagnetic Mode) at a transmission frequency of 10.6 microns.

The beam was defocused at the specimen to a diameter of approximately 3 mm to yield an incident average power density of approximately 1.25 Kw/cm<sup>2</sup> absorbed by the specimen. A coincident helium-neon laser was used to provide a visible red beam for alignment of the "hot" CO<sub>2</sub> laser beam on the titanium airfoil. Observation of this red alignment beam was accomplished using the video tape system which permitted either monochrome or color position readout.



FD 127300

*Figure 2. Titanium Combustion Test Rig*



FD 124486

*Figure 3. Titanium Combustion Rig Test Section*

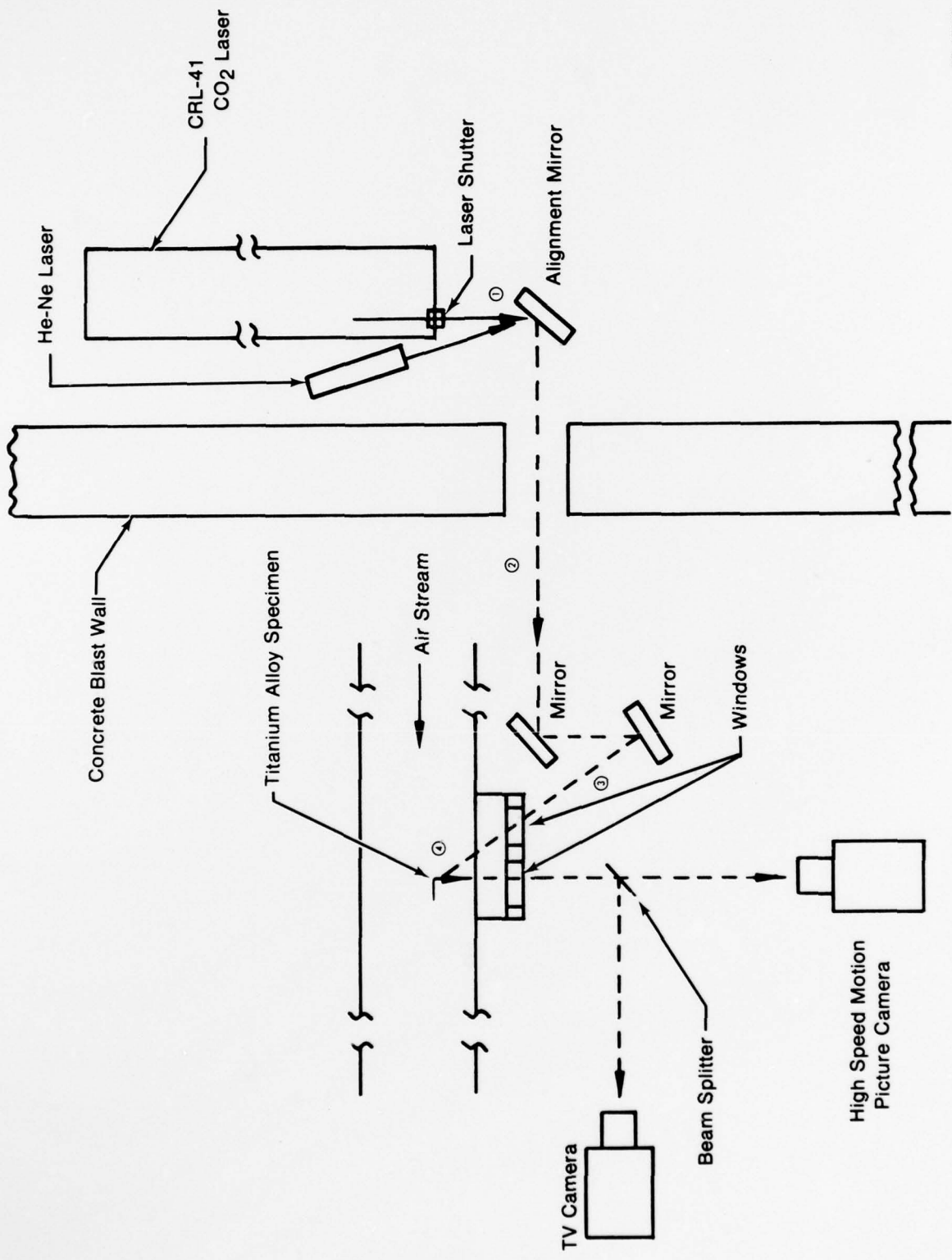
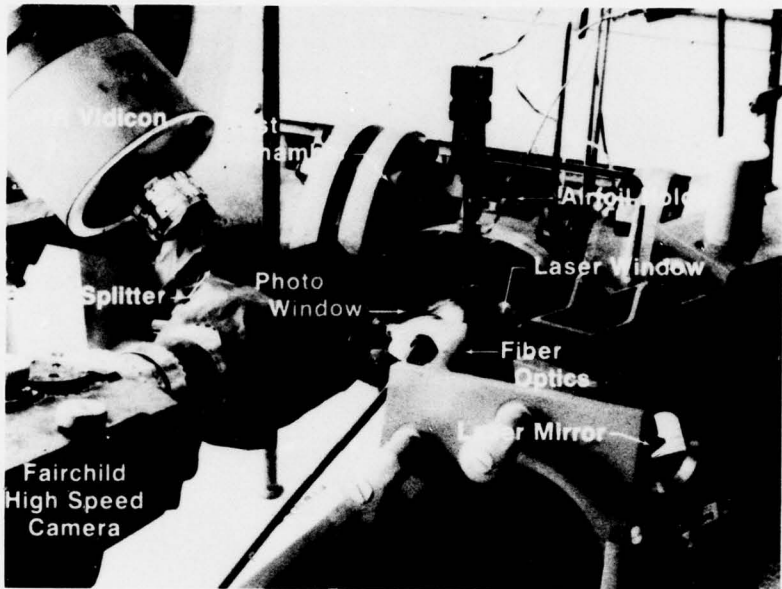


Figure 4. Arrangement of Laser Ignition and Photographic Recording Systems

FD 124487



FC 42608A

*Figure 5. Laser Airfoil Ignition Test Rig*

#### TEST PROCEDURE

Laser ignition was employed to initiate the severe reaction required to ignite the titanium alloy specimens. Prior to the test runs a determination was made of the laser power available to the specimen. Table 1 lists the power, in watts, at significant points from the laser shutter to the specimen location. Figure 4 shows the locations of these points.

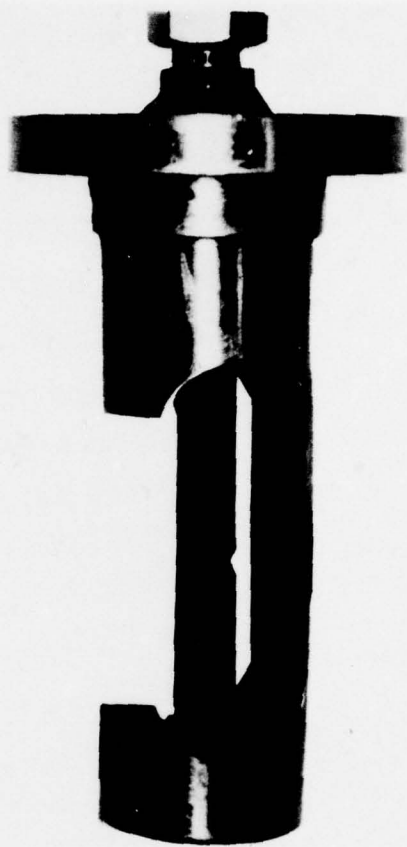
**TABLE 1. LASER POWER LOSSES OBSERVED IN THE TITANIUM COMBUSTION TEST**

<i>Laser Power Monitored (Watts)</i>	<i>Cumulative Loss From Head To Location (%)</i>	<i>Location of Water Cooled Monitor</i>	<i>Figure 4 Marker</i>
225	0	Before Alignment Mirror	(1)
175	22	After Alignment Mirror	(2)
150	33	After Rig Mirror "Pair"	(3)
130	42	After Laser (ZnSe) Window	(4)

In a separate determination, the laser energy absorbed by the leading edge of a titanium specimen coated with black nickel was shown to be 61%.

These preliminary energy output/coupling tests indicated that 35.4% of the laser output energy was available for ignition of the specimen. For all test runs, laser energy was applied to the specimen midpoint leading edge for a period of 5 seconds.

The test sequence employed in this program evolved from experience gained during previous test programs. Each test run began by securing the test specimen in the specimen holder (Figure 6) which was then mounted in the test chamber.



FD 124488

*Figure 6. Test Specimen in Holder*

Individual run values for air velocity and pressure were established by installing a specific combination of the flow measuring orifice and the back pressure orifice in the test rig.

After setting the heater to the desired temperature, airflow was introduced into the system and the test chamber allowed to come to thermal equilibrium. The time required to stabilize depended on the amount of temperature change from the previous test point. From a cold start condition this could be up to 30 minutes. At thermal equilibrium, the laser optics were aligned using the visible helium-neon laser and the video tape system. Specimen illumination during this alignment was provided by light transmitted from its source by fiber optics. For high speed photographic coverage the camera was focused on the specimen at all times during the run. No external light was used during the high speed photography. Light from the specimen ignition and burning was sufficiently intense to permit photo documentation of burning rates and melt transport. An event marker (light pulse) was recorded on the left side of the film on all runs to annotate the start and finish of the laser action during the run. The high speed films were also marked with light pulses from a 1000 Hertz timing generator to provide an absolute time reference for event sequences.

Just prior to start of run a final check/adjustment was made of laser alignment and run parameters which were recorded. The test run was initiated by an electronic, time-sequenced switch which, when actuated, started the high speed camera and video tape recorder. Approximately 2 seconds after camera start the laser shutter opened to irradiate the specimen thereby starting the run. The laser was "on" for 5 seconds before the sequencer closed the shutter and stopped the photographic and video cameras.

### SECTION III

#### TEST RESULTS AND ANALYSIS

##### TEST DATA

Table 2 contains the pretest data on specimen weight, width and midspan thickness along with test run environmental test chamber conditions of temperature, pressure and air velocity. Also included is the laser head output power for each run.

TABLE 2. SPECIMEN INITIAL DATA AND RUN CONDITIONS

Alloy	ID Number	Specimen			Run Conditions				
		Width (mm)	Thickness at Midchord (mm)	Temperature °C (°F)	Pressure MPa (psia)	Air Velocity m/sec (ft/sec)	Laser Head Power (watts)		
		(in.)	(in.)						
Ti 13-11-3	1-1	24.77 (0.975)	1.367 (0.0538)	427 (800)	0.48 (70)	237 (778)	265		
Ti 13-11-3	1-2	24.89 (0.980)	1.501 (0.0591)	207 (405)	0.61 (89)	118 (386)	260		
Ti 6-4	2-1	24.97 (0.983)	1.361 (0.0536)	429 (804)	0.49 (71)	240 (789)	265		
Ti 6-4	2-2	25.10 (0.988)	1.438 (0.0536)	209 (408)	0.61 (89)	113 (371)	255		
Ti 6-6-2	3-1	22.86 (0.900)	0.950 (0.0374)	427 (800)	0.48 (70)	238 (782)	265		
Ti 6-6-2	3-2	22.56 (0.888)	1.021 (0.0402)	206 (402)	0.62 (90)	113 (370)	260		
Ti 6-2-4-2	4-1	23.50 (0.925)	1.085 (0.0427)	424 (796)	0.48 (70)	237 (777)	265		
Ti 6-2-4-2	4-2	23.50 (0.925)	1.054 (0.0415)	207 (404)	0.62 (90)	113 (370)	260		
Ti 6-2-4-6	5-1	24.92 (0.981)	1.433 (0.0564)	429 (804)	0.48 (70)	235 (771)	265		
Ti 6-2-4-6	5-2	24.92 (0.981)	1.516 (0.0597)	202 (396)	0.62 (90)	114 (374)	260		
Ti 8-1-1 W/IVD	B-1	24.92 (0.981)	1.374 (0.0541)	429 (804)	0.48 (70)	238 (782)	265		
Ti 8-1-1 W/IVD	B-2	25.02 (0.985)	1.422 (0.0560)	207 (404)	0.61 (89)	113 (371)	250		
Ti 3 Al	A-1	26.72 (1.052)	1.118 (0.0440)	429 (804)	0.48 (69)	244 (799)	265		
Ti 3 Al	A-2	26.44 (1.041)	1.143 (0.0450)	207 (404)	0.62 (90)	115 (378)	260		
Ti 13 Cu	1-Cu	25.10 (0.988)	1.252 (0.0493)	426 (798)	0.48 (69)	245 (803)	265		
Ti 13 Cu	2-Cu	25.15 (0.990)	1.245 (0.0490)	208 (406)	0.62 (90)	115 (376)	260		
Ti 6-2-4-2 W/CM	4CM3	23.88 (0.940)	1.052 (0.0414)	430 (806)	0.49 (71)	233 (765)	265		
Ti 6-2-4-2 W/CM	4CM4	23.98 (0.944)	1.019 (0.0401)	210 (410)	0.62 (90)	115 (378)	260		
Ti 8-1-1 W/CM	6CM1	24.92 (0.981)	1.351 (0.0532)	429 (804)	0.48 (70)	238 (781)	265		
Ti 8-1-1 W/CM	6CM2	25.10 (0.988)	1.369 (0.0539)	207 (404)	0.61 (89)	111 (364)	250		
Ti 8 Mn	11-1	21.74 (0.856)	0.676 (0.0266)	429 (804)	0.48 (70)	241 (790)	265		
Ti 8 Mn	11-2	22.38 (0.881)	0.775 (0.0305)	206 (402)	0.63 (91)	115 (376)	260		
Ti 8-1-1	51-0	25.20 (0.992)	1.466 (0.0577)	202 (395)	0.62 (90)	112 (367)	250		
Ti 8-1-1	6-1	24.94 (0.982)	1.369 (0.0539)	432 (810)	0.48 (70)	232 (762)	260		
Ti 13 Cu - 1.5 Al	3 Cu	24.82 (0.977)	1.257 (0.0495)	431 (808)	0.62 (90)	236 (773)	265		

The environmental run conditions of temperature, pressure and air velocity were established by using various combinations of flow control and back pressure orifice plates. The finite number of orifice plates available together with their interactive effect on run parameters, however, produced some variation from desired set conditions. Temperature and pressure variations were minimum and within acceptable limits (approximately  $\pm 2\%$ ). Although air velocity values all exceeded the desired run point of 213 m/sec (700 ft/sec) by from 9 to 15%, the total variation within the range achieved was only about 5%.

Specimen dimensional variations were more significant. Because of the specimen airfoil configuration and tracer machining difficulties, a range greater than 2:1 was found in the midchord thickness.

Table 3 is a tabulation of test run results and the subsequently calculated measures of specimen performance. Figures 7 and 8 show the postrun appearance of the test specimens. For the purpose of understanding Table 3, the following definitions of columnar headings are provided:

No Damage: This category included those specimens receiving a heat input rate via laser less than or equilibrated with the combined heat loss rate from conduction, convection and radiation processes.

Notch: Energy input from the laser was sufficient, in these cases, to ignite the specimens over some limited area, however, the energy being generated from the combustion process was less than the combined heat losses so the burning processes ceased before reaching midspan.

Burn: The specimen ignited and sustained combustion propagated across the width of the airfoil.

Ignition Time: This is defined as the time in seconds required for the laser beam impingement on the specimen to produce visible signs of a melt condition.

Average Burn Rate: This is defined as the total weight (grams) of metal lost, through burning, per second of total burn time. For this definition, total burn time is the interval between inception of burning (time of first visible melt) to end of burn (absence of visible melt).

Time to Burn-Through: This is the interval between ignition and the time that burning has severed the specimen.

Burn Severity: This is defined as the percent of the exposed area which was burned. Original exposed area excludes that portion secured in the specimen holder.

Low Temperature Condition: This will be used in the ensuing discussion when referring to test chamber conditions of 240 °C (400°F) (temperature), 0.62 MPa (90 psia) (pressure) and 122 m/sec (400 ft/sec) (air velocity).

High Temperature Condition: This will be used in the ensuing discussion when referring to test chamber conditions of 427°C (800°F) (temperature), 0.48 MPa (70 psia) (pressure) and 213 m/sec (700 ft/sec) (air velocity).

Primary time data for ignition, burn-through and total burn time was extracted from the high speed photographic film by visual inspection. Although the film was accurately annotated every millisecond, the occurrence of a given event, such as the recognition of the start of melt, was somewhat subjective. It is estimated that the primary time data could be in error by a maximum of 10 milliseconds and is a relatively constant quantity not related to the absolute magnitude of the value.

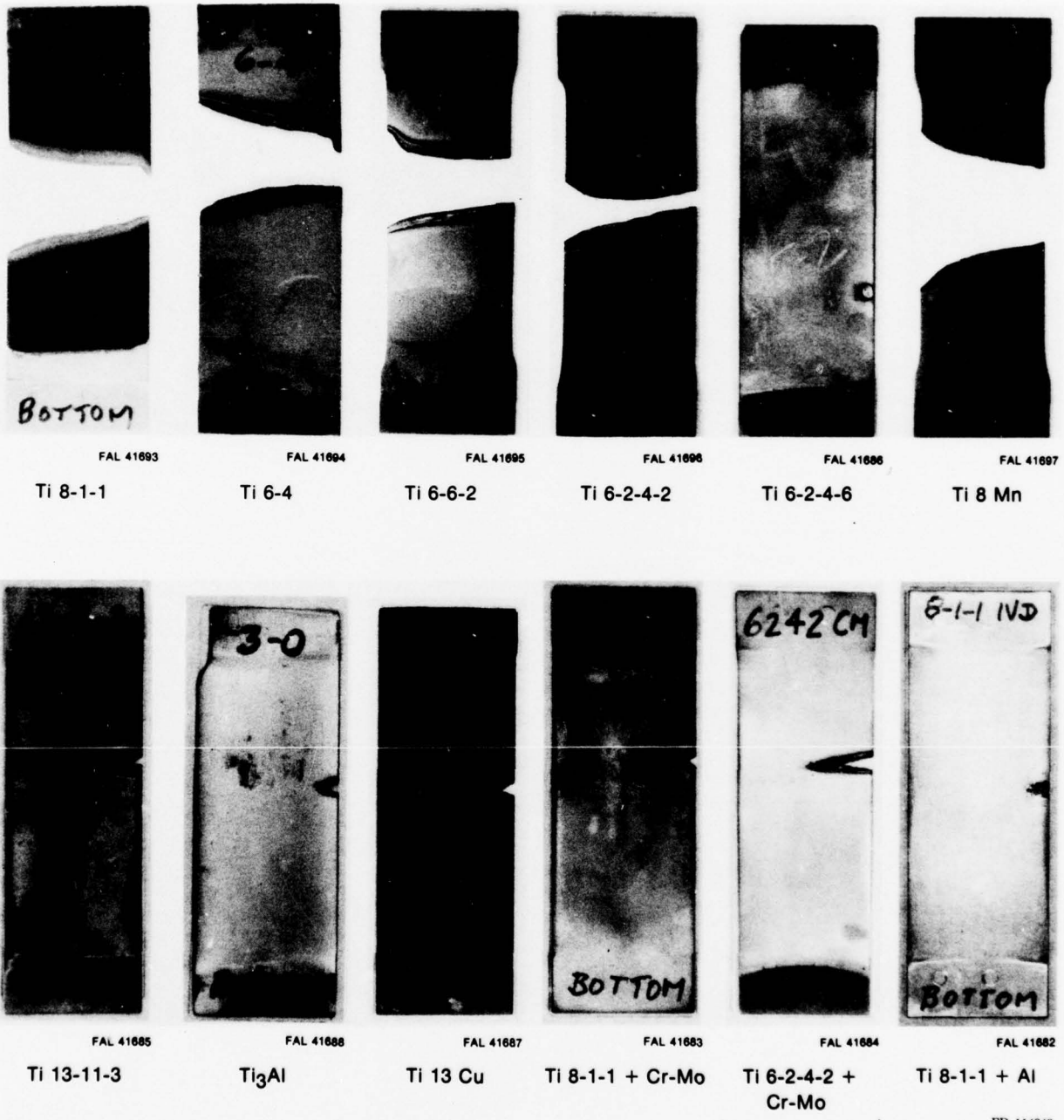
For burn severity calculation, burn area was measured with a planimeter using photographs of the reconstructed (lengthwise) specimen. The potential error of this measurement is estimated to be approximately  $\pm 2$  to 5%.

TABLE 3. SPECIMEN TEST DATA AND RESULTS

Alloy	Specimen ID	Reaction to Laser	Time to Burn-Through (sec)	Ignition Time (sec)	Weight Lost During Burn (g)	Total Burning Time (sec)	Average Burn Rate (g/sec)	Burn Severity (%)
								213 m/sec (90 psia)
Ti 13-11-3	1-1	Notch	—	0.247	—	—	—	—
Ti 6-4	2-1	Burn	0.435	0.294	3.9813	3.446	1.16	48
Ti 6-6-2	3-1	Burn	0.343	0.187	1.2730	3.153	0.40	31
Ti 6-2-4-2	4-1	Burn	0.358	0.149	2.3075	3.140	0.74	48
Ti 6-2-4-6	5-1	Burn	0.411	0.420	8.8629	5.465	1.62	87
Ti 8-1-1 W/IVD	B-1	No damage	—	—	—	—	—	—
Ti 3 Al	A-1	Notch	—	0.367	—	—	—	—
Ti 13 Cu	1-Cu	No damage	—	—	—	—	—	—
Ti 6-2-4-2 W/CM	4CM3	Burn	0.354	0.179	0.8515	0.981	0.87	19
Ti 8-1-1 W/CM	6CM1	Burn	0.476	0.270	4.3619	2.830	1.54	53
Ti 8 Mn	11-1	Burn	0.267	0.147	0.9804	1.366	0.72	37
Ti 13 Cu - 1.5 Al*	3 Cu	Burn	0.857	0.230	3.1905	3.880	0.82	16
Ti 8-1-1	6-1	Burn	**	**	6.1439	**	**	84
Ti 13-11-3	1-2	Notch	—	0.649	—	—	—	—
Ti 6-4	2-2	Burn	0.913	0.175	1.4958	3.072	0.49	26
Ti 6-6-2	3-2	Burn	0.582	0.147	0.8150	1.830	0.45	21
Ti 6-2-4-2	4-2	Burn	0.676	0.133	0.3764	1.426	0.26	17
Ti 6-2-4-6	5-2	No damage	—	—	—	—	—	—
Ti 8-1-1 W/IVD	B-2	Hole	—	0.570	—	—	—	—
Ti 3 Al	A-2	Notch	—	0.178	—	—	—	—
Ti 13 Cu	2-Cu	Notch	—	0.187	—	—	—	—
Ti 6-2-4-2 W/CM	4CM4	Notch	—	0.200	—	—	—	—
Ti 8-1-1 W/CM	6CM2	Notch	—	0.188	—	—	—	—
Ti 8 Mn	11-2	Burn	0.499	0.158	1.0250	1.376	0.74	32
Ti 8-1-1	51-0	Burn	0.867	0.125	1.5224	1.995	0.76	25

\*Run at 0.62 MPa (90 psia).

\*\*Camera Problem — no photo coverage.



*Figure 7. Appearance of Test Specimens After Laser Impingement in 240°C (400°F), 0.62 MPa (90 psia), 122 m/sec (400 ft/sec) Airstream*

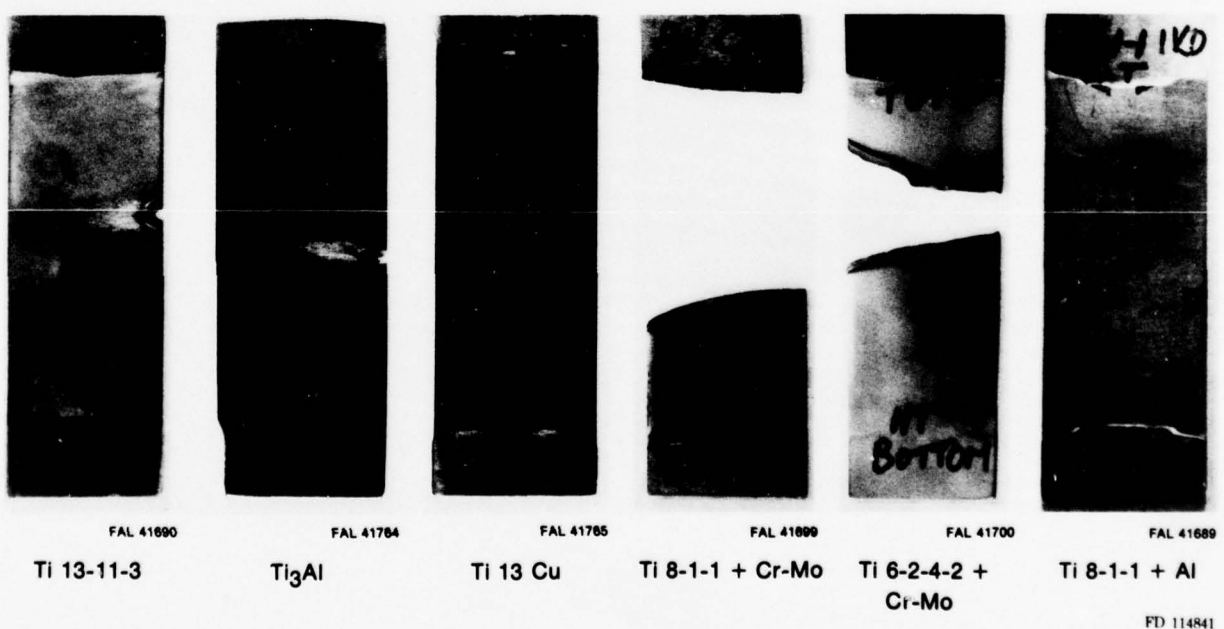
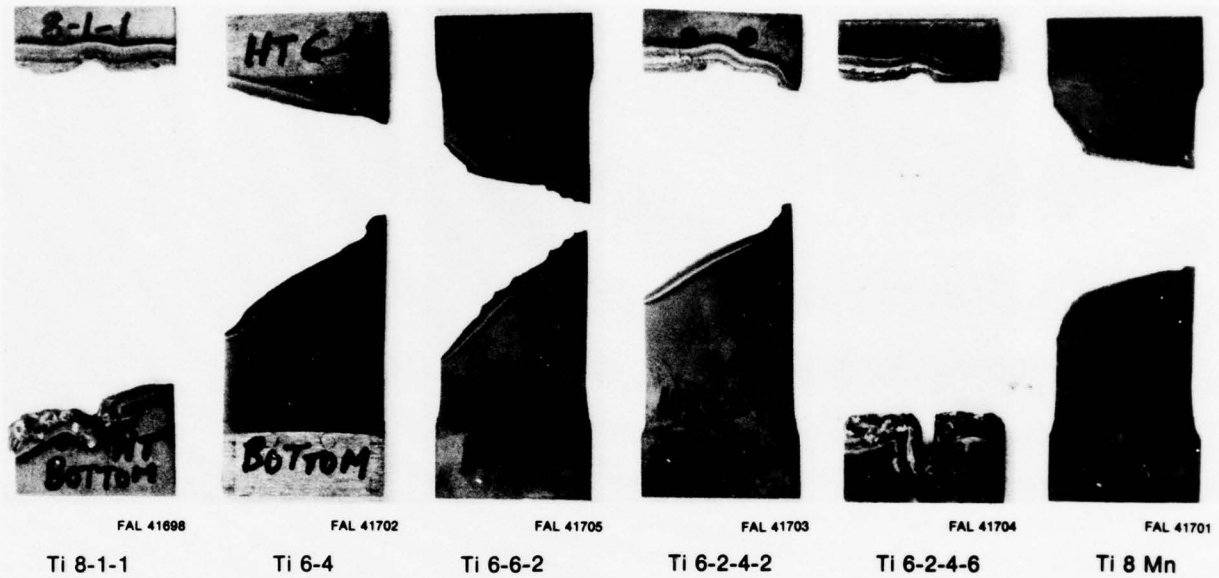


*Figure 8. Appearance of Test Specimens After Laser Impingement in 427°C (800°F), 0.48 MPa (70 psia), 213 m/sec (700 ft/sec) Airstream*

## **ANALYSIS OF TEST DATA**

Of the 25 test runs performed, the laser beam failed to damage 3 specimens (except for minor heat discoloration), produced a notch in 7, burned 14 and, in 1, burned a small hole (approximately 3 mm in diameter) at the point of laser impingement.

Failure of the three specimens to experience damage must be attributed to an inadequate quantity of laser power reaching the specimen. Since laser output power was measured as adequate for all test runs, failure to produce an effect on these specimens was due to a degraded transmission of the laser beam through the zinc selenide window. This latter effect can occur when the laser beam encounters an obstacle (to transmission) on the zinc selenide window caused by metal splatter damage during previous runs.

### **Ignition**

Ignition time, the time to visible evidence of first melt which subsequently resulted in sustained combustion, was considered to be a measure of the ignition properties of the specimens tested. Although the specimens did show a significant variation in this time element, these same specimens also exhibited an equally significant variation in the leading edge thickness at the point of laser impingement. In an attempt to understand the relationship between this thickness at a point 0.05 inch from the leading edge (laser "hit" point) and the laser effect on the specimen, Table 4 was constructed.

**TABLE 4. THE RELATIONSHIP BETWEEN SPECIMEN THICKNESS AND LASER EFFECT**

<i>Laser Effect on Specimen</i>	<i>Number of Specimens</i>	<i>Leading Edge Thickness Range mm(in.)</i>
No Damage*	4	0.599 to 0.762 (0.0236 to 0.0300)
Notch	7	0.556 to 0.800 (0.0219 to 0.0315)
Burn	13	0.0116 to 0.0277

Note: \* Includes specimen B-2 which experienced a small (laser beam diameter) hole.

An inspection of the thickness ranges shown on Table 4 indicates that the minimum and maximum thickness specimens were in the groups representing a laser effect of *notch* and *burn*. This would tend to indicate that laser power was adequate to produce a melt and thus effect ignition on even the thickest specimen and therefore those experiencing *no damage* did so because of inadequate laser energy reaching the specimen due to transmission obstacles. An inspection of Table 3 shows that ignition time was generally longer at the high temperature condition. This was due to the higher air velocity which removed incident heat (from the laser beam) at a greater rate (than at the low temperature condition).

### **Combustion Characteristics**

Burn severity ranking for those specimens experiencing sustained combustion is shown on Figures 9 and 10. These figures establish that burning was more severe at the high temperature condition than the low temperature condition. In addition the extent to which a given alloy burns at each of the two conditions varies considerably among the alloys. If the ratio of burn severity at the high temperature condition to that at the low temperature condition is calculated for those alloys common to the two conditions, the results produce a range from 1.16 for Ti 8Mn to 3.36 for Ti 8-1-1. Previously expressed concern over specimen thickness variation does not affect this calculation since specimens of a given alloy had essentially equal thicknesses. Thus the burning of Ti 8Mn is affected very little by increasing the severity of the environment while Ti 8-1-1 is very significantly affected. This alloy combustion characteristic is not fully understood.

The identification of alloy effect on combustion at a given environmental condition required the elimination of the possible compounding effect of specimen thickness variations. This was done by comparing the alloys in essentially equal-thickness groups.

At the low temperature condition alloys Ti 6-6-2 and Ti 6-2-4-2 had approximately equal thickness [1.02 mm (0.04 in.)] and experienced 21% and 17% burn severity respectively. Although these values may not appear to represent a significant difference, the appearance of the reconstructed specimens (Figure 9) would tend to establish that, at this environmental condition, Ti 6-2-4-2 is more resistant to burning. At these same conditions alloys Ti 6-4 and Ti 8-1-1 had equal thicknesses [1.45 mm (0.057 in.)] and had burn severity values of 26 and 25% respectively. This difference is not significant thereby indicating that Ti 6-4 and Ti 8-1-1 burn equally at the low temperature condition.

At the high temperature condition equal thickness considerations, after eliminating coated alloys, yielded only one group. This group consisted of alloys Ti 6-2-4-6, Ti 8-1-1 and Ti 6-4 having equal thicknesses of approximately 1.27 mm (0.05 in.) and burn severity performance of 87, 84 and 48% respectively. The difference between Ti 6-2-4-6 and Ti 8-1-1 indicated essentially equal burn severity. Ti 6-4, however, very significantly was more resistant to extensive burning than the other two. Thus, although Ti 6-4 and Ti 8-1-1 burned to the same degree at the low temperature condition, at the high temperature condition the environmentally related increase in burn severity for the Ti 6-4 was significantly less. Expressed in terms of burn severity ratio (as defined in the first paragraph), Ti 6-4 had a lower ratio (1.85) than Ti 8-1-1 (3.36).

Figure 11 shows a plot of the combustion front travel across the specimen as a function of time after ignition for each burned alloy at the two environmental conditions. These curves illustrate that at the high temperature condition the alloys burn faster and that the time-to-burn-through range is smaller than at the low temperature condition. Of greater significance, however, is the broader spread of burn-through time at the low temperature condition. This broader spread amplifies the alloy or thickness effect on burn propagation rate as is illustrated by the relationship of Ti 6-6-2 and Ti 6-2-4-2 at the two conditions. At the high temperature condition these alloys burned-through in the same interval whereas at the low temperature condition they exhibited an appreciable separation.

**Low Temperature Condition (400°F - 90 psia - 400 ft/sec)**

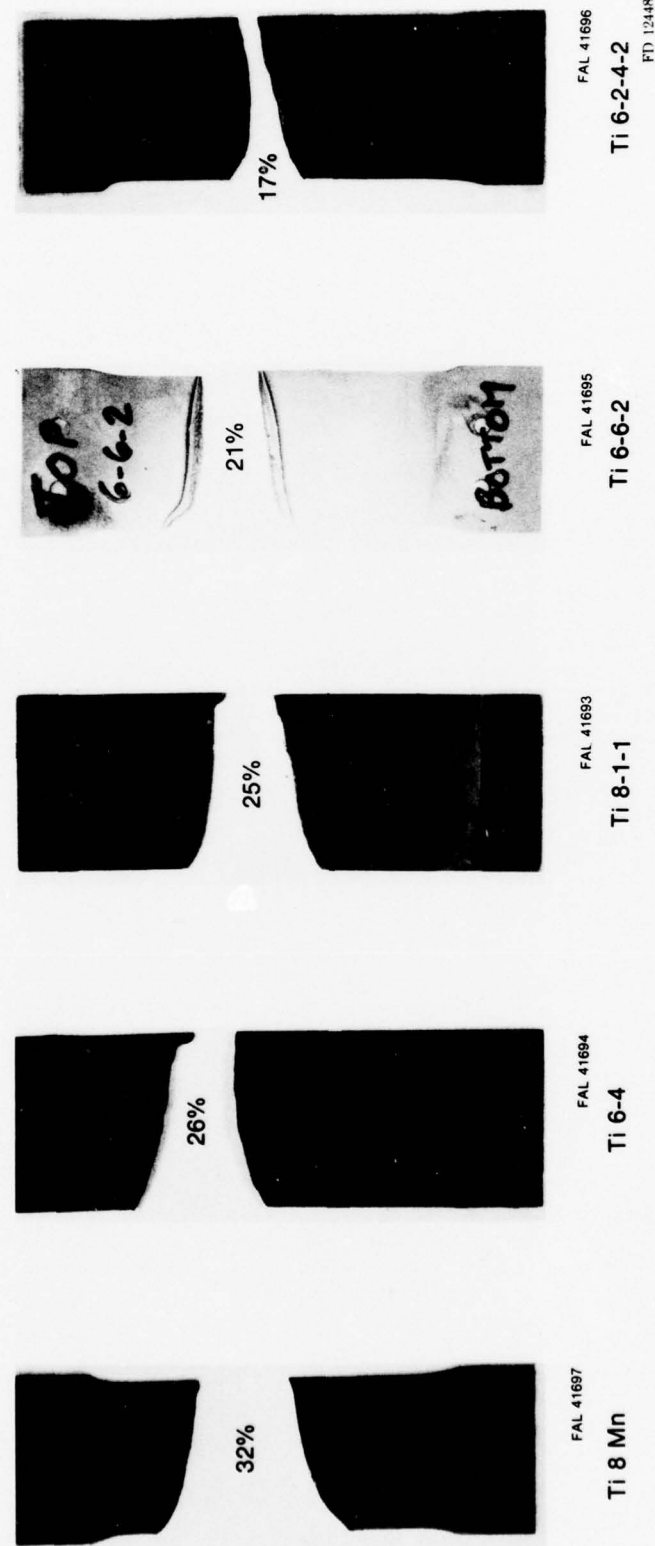


*Figure 9. Test Alloys Ranked by Burn Severity (Percent of Exposed Area Burned)*

**High Temperature Condition (800°F - 70 psia - 700 ft/sec)**

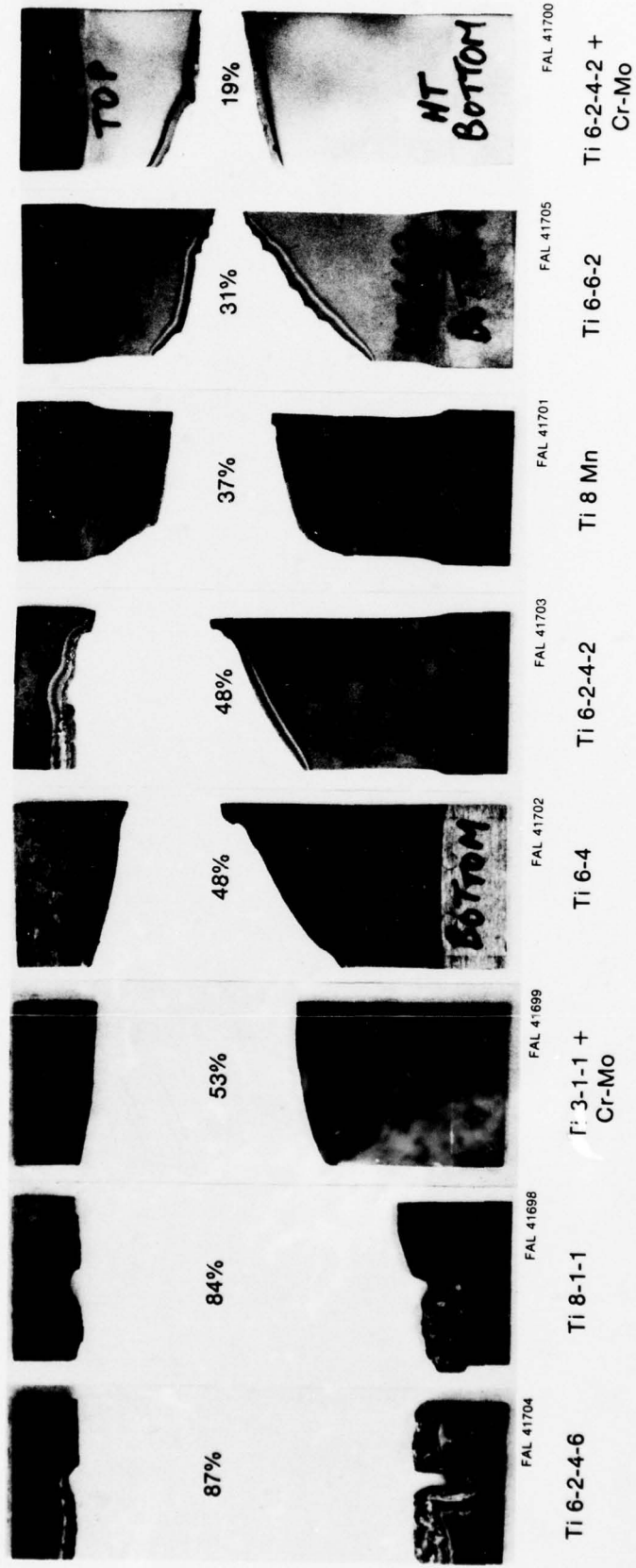


*Figure 10. Test Alloys Ranked by Burn Severity (Percent of Exposed Area Burned)*

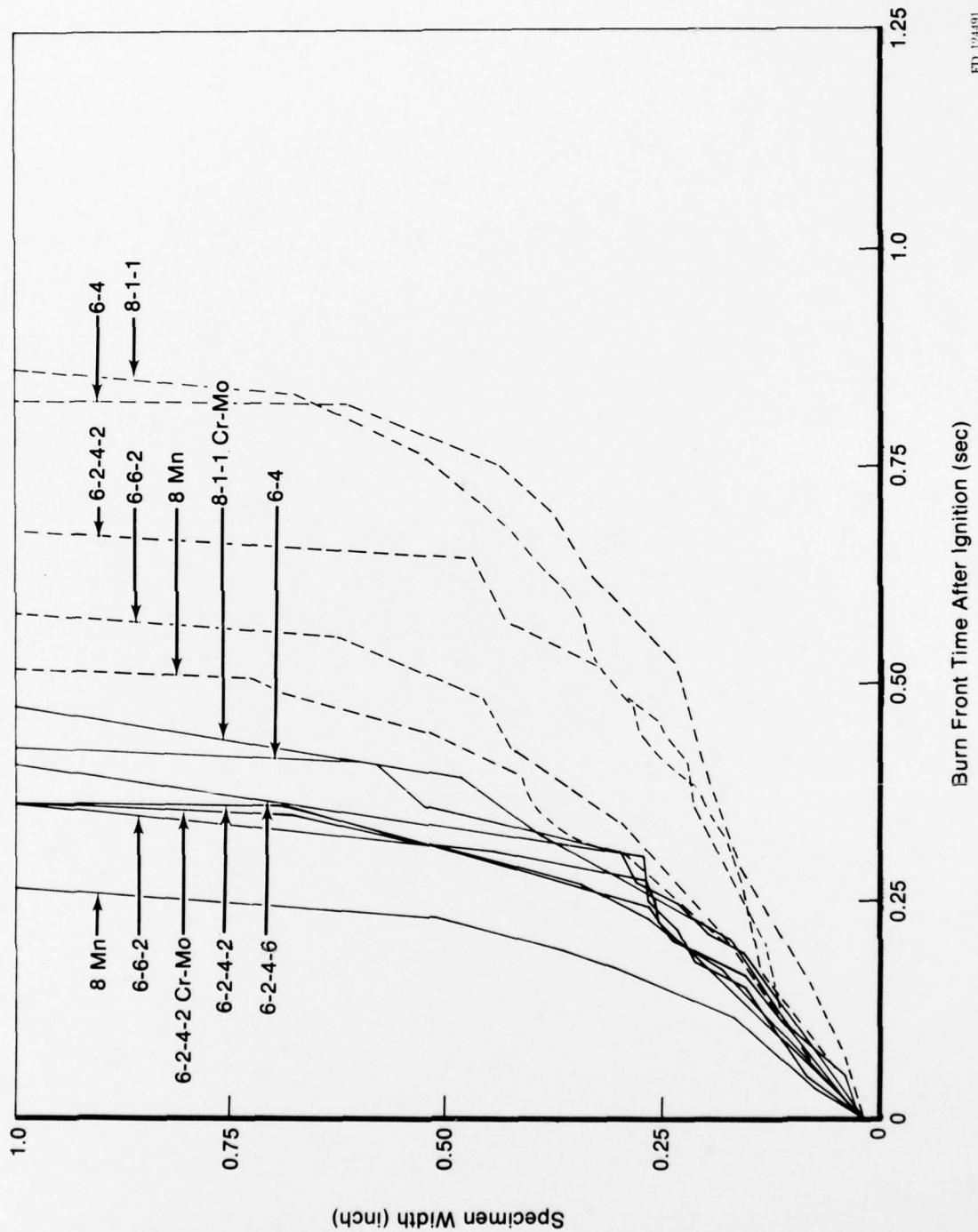


Figure 11. Time-Distance Travel of Combustion Front

FD 124491

### **Specimen Coating Effect**

A comparison of the test performance of Ti 6-2-4-2 and Ti 6-2-4-2 coated with chromium-molybdenum at the high temperature condition showed no apparent difference in ignition time. Although the specimen with chromium-molybdenum coating did take 0.014 second longer to ignite, it was also approximately 35% thicker at the point of laser hit. This condition would tend to offset the ignition time increase. Once ignited both the coated and uncoated alloy burned through the specimen in the same amount of time. After severing the specimen, the uncoated Ti 6-2-4-2 continued burning in a direction at right angles to the airflow for a significantly longer time than the chromium-molybdenum coated specimen. The burn severity of the uncoated Ti 6-2-4-2 (48%) was 2½ times that of the coated specimen (19%).

At the low temperature condition the Ti 6-2-4-2 with chromium-molybdenum coating was only notched and thus permitted no direct comparison with the burned, uncoated Ti 6-2-4-2. The notch, however, did extend approximately 20% of the distance across the specimen. This is well beyond the laser hit point and thus it must be concluded that a limited sustained burning occurred. Extinguishment of the burn at this point must be attributed to the influence of the chromium-molybdenum coating. Figure 12 shows high-speed film frames of the combustion propagation of the uncoated Ti 6-2-4-2 and the notch formation of the Ti 6-2-4-2 with chromium-molybdenum coating.

The Ti 8-1-1 specimen coated with IVD aluminum experienced a small hole (laser beam diameter) at the low temperature condition. This indicates that the laser power was adequate to cause a melt condition at the point of impingement. The low melting temperature, high thermal conductivity and/or high heat of fusion of the aluminum coating, however, prevented a sufficient amount of the titanium substrate from reaching melt temperature as required for sustained combustion. At the high temperature condition the specimen experienced no damage. This occurrence must be attributed to a lack of adequate energy reaching the specimen caused by laser beam transmission obstacles on the Zn Se laser window.

A problem with the high-speed camera resulted in the loss of the photographic record (and thus the time data) of the ignition and burn of the uncoated alloy Ti 8-1-1 at the high temperature condition. However, data on burn weight loss and area of burn from other sources was available to base generalized conclusions. At the high temperature condition, both the uncoated Ti 8-1-1 and the chromium-molybdenum coated specimens experienced sustained combustion. The uncoated Ti 8-1-1 lost 60% of its original weight upon burning whereas the chromium-molybdenum coated specimen lost 43%. Burn severity was 84% for the uncoated and 53% for the chromium-molybdenum coated specimens.

At the low temperature condition the uncoated Ti 8-1-1 ignited and sustained combustion to yield a nominal 25% burn severity. The chromium-molybdenum coated Ti 8-1-1, however, only suffered a notch which did not progress appreciably beyond the laser "hit" point.

In summary, uncoated Ti 8-1-1 ignites rather easily and burns to an extent consistent with the severity of the environmental test conditions. In addition it was shown that a chromium-molybdenum coating had a pronounced effect on reducing or preventing ignition and, additionally, if ignited, it significantly reduced the severity of burning. IVD aluminum was shown to be capable of protecting Ti 8-1-1 from ignition under the environmental conditions tested.

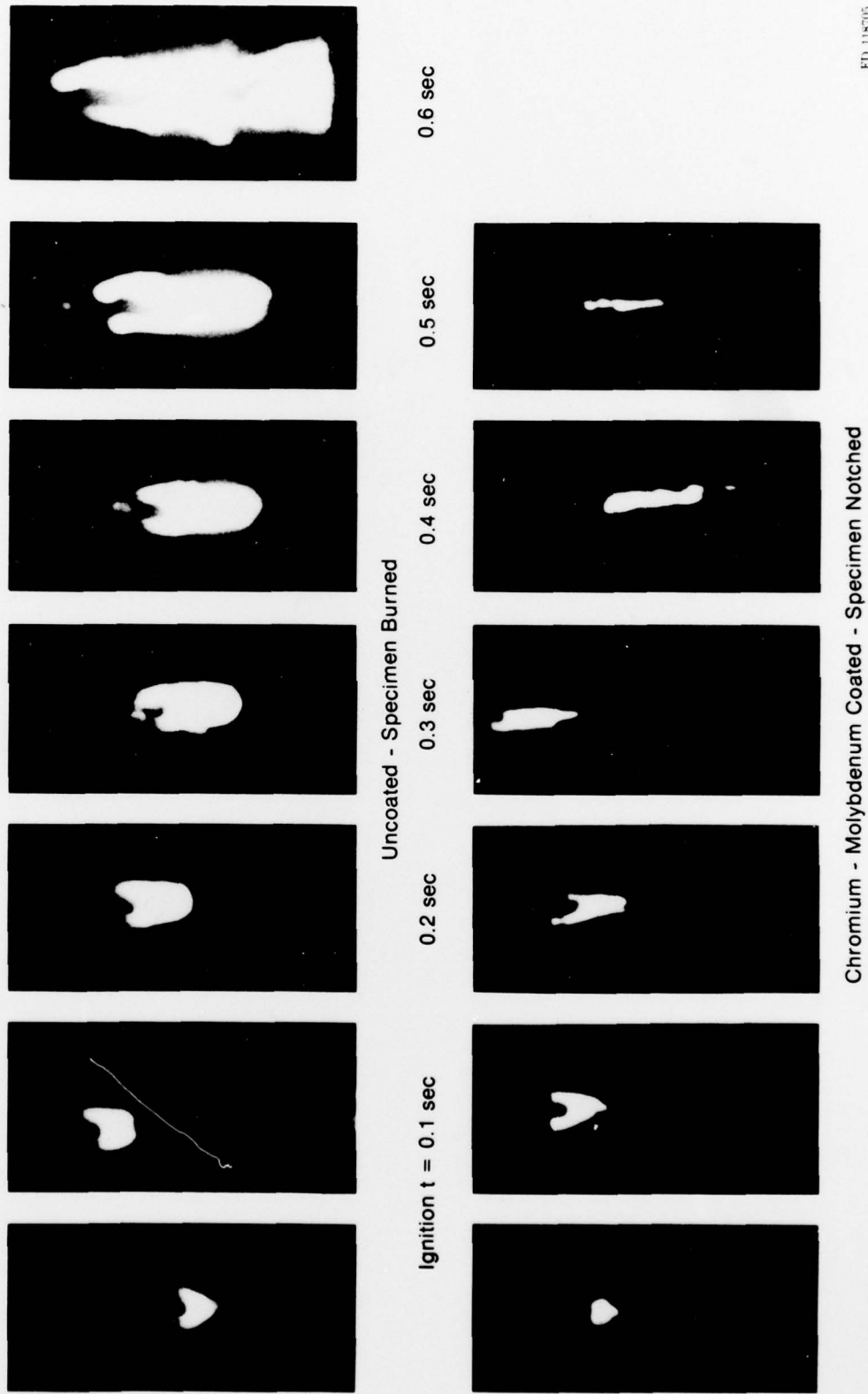


*Figure 12. Burn Propagation of Coated and Uncoated Ti 6-2-4-2 at Low Temperature Condition*

### Metallographic Examination Results

Metallographic cross sections of some of the burned specimens were prepared and used to study temperature distribution into the specimen which resulted from the molten burning titanium. A light microscope was used to study overall microstructural changes and a scanning electron microscope was used to measure distances from the original metal surface to the farthest point which had exceeded the beta transus temperature. The depth of "heat affect" was also determined with the scanning electron microscope. These results are summarized on Table 5. Figure 13 shows how these cross sections were used on a chromium-molybdenum coated Ti 6-2-4-2 specimen.

TABLE 5. DEPTHS OF MICROSTRUCTURAL CHANGES FROM METALLOGRAPHIC EXAMINATION

Alloy	Results From Low Temperature Test			Results From High Temperature Test		
	Depth, $\mu$ , of		No Microstructural Change	Depth, $\mu$ , of		No Microstructural Change
	Recast	Beta Transus Exceeded		Recast	Beta Transus Exceeded	
Ti 8-1-1	40	800	1670	150	2200	5350
Ti 6-4	10	1300	1720	30	1500	1950
Ti 8Mn	90	900	4100	120	1320	2700
Ti 6-2-4-2	40	1200	1800	—	—	—
Ti 8-1-1 (Cr-Mo Coat)	10	650	1200	70	500	1040
Ti 6-2-4-2 (Cr-Mo Coat)	10	650	1200	—	—	—

From previous literature (References 3 and 4), the temperature at the surface of the molten metal could range from 1593°C (2900°F) to 2982°C (5400°F). Since this surface point is not well defined (the actual location being above the original titanium surface, on the surface of the flowing molten metal) it will not be used in the analysis. The remelt layer had to be at the melting temperature of titanium, about 1704°C (3100°F), and, therefore, it provides one point of reference to study the metallographic results. Large beta grains, formed in regions where the specimen temperature exceeded the beta transus temperature of about 954°C (1750°F), yields a second temperature reference point at that severely heat affected zone. The point in the base metal where the elevated temperature had caused a discernible microstructural change is assumed to have reached a minimum of 704°C (1300°F). This provides a third temperature reference point.

The temperature-vs-depth values summarized on Table 5 cannot be used as accurate representations of temperatures or even relative temperatures within the different alloy systems. The kinetics of phase transformations for these short time-at-temperature exposures have not been studied and probably vary for different alloys. We can, however, arrive at some understanding of alloy temperature distribution, caused by fire, from this type of analysis. The expected variations are minimized when comparing a given alloy at different environmental conditions or a given alloy coated and uncoated. This type of comparison is shown on Figures 14 and 15. In these cases, since the structural transformation kinetics are identical for identical alloys, when a greater heat-effected distance from the burning tip is observed it must have resulted from one or more of the following factors:

1. More heat is generated during combustion, i.e., a greater percentage of the metal reacted to form the oxide.
2. More energy was coupled into the specimen. This will encompass factors such as wettability, amount of metal blown off of the surface, and liquid/solid interfaces restricting heat flow into the base metal.
3. Reduced surface conduction of heat.

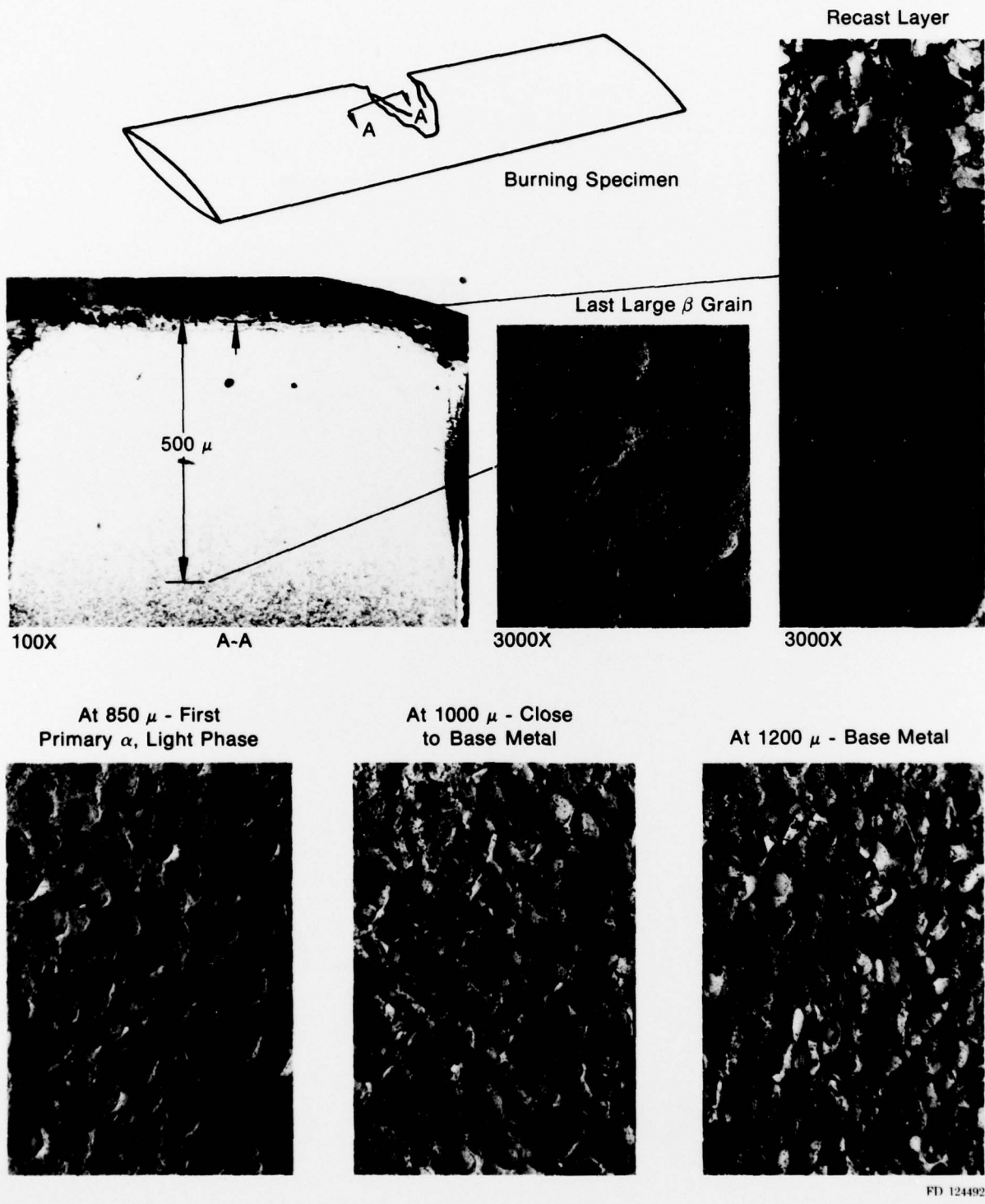


Figure 13. Metallographic Examination of Chromium-Molybdenum Coated Ti 6-2-4-2 After Testing Under Low Temperature Conditions

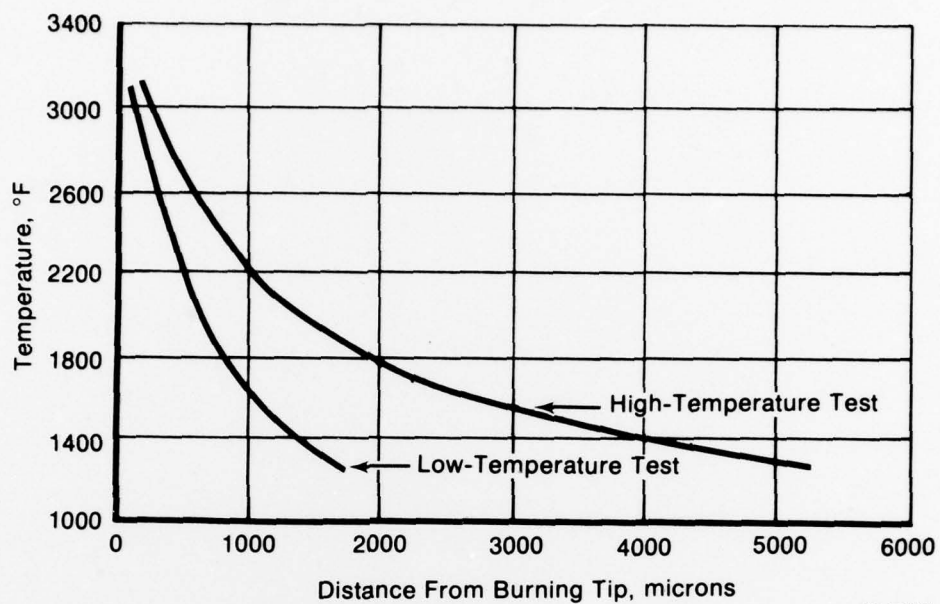


Figure 14. Effect of Test Conditions On Temperature Distribution in Ti 8-1-1

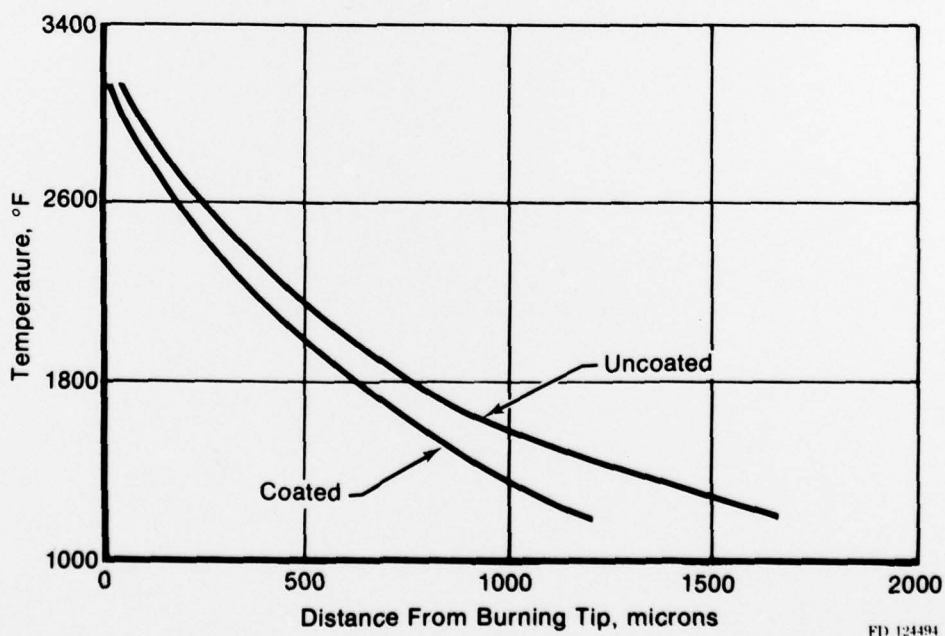


Figure 15. Effect of Coating on Temperature Distribution in Ti 8-1-1

The differences observed in the two test conditions shown on Figure 14 support the previous observations that a more energetic reaction (more heat generated) occurred at the higher temperature condition as evidenced by a deeper heat-affect zone. Since higher velocities were used at the higher temperature conditions, energy coupling should have been reduced. This would have had the opposite effect on temperature distribution as influenced by test conditions. Differences in surface conduction would not occur by changing the environmental test conditions.

The chromium-molybdenum coating was shown to reduce the depth of heat-affected metal (Figure 15 and Table 5). A combination of increased surface conduction with decreased energy coupling most likely caused these observed affects. This decreased energy coupling is vividly depicted on the high speed film frames shown on Figure 12.

## **SECTION IV**

### **ANALYTICAL SIMULATION**

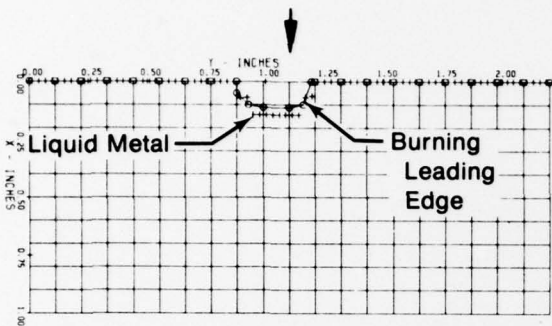
An extensive program of analytical and experimental investigation has been in progress for the past 2 years under separate contract (Reference 5) to establish the environmental parameters which govern the ignition and self-sustained combustion of two titanium alloys (Ti 6Al-4V and Ti 8Al-1Mo-1V) over a range of aerodynamic environments. An analytical model is being evolved to predict the ignition and subsequent self-sustained combustion of titanium alloys. Numerical finite-difference techniques are used to produce simultaneous solutions of the equations for heat and mass transfer in the aerodynamic boundary layer, transient thermal conduction in the solid metal, phase change and liquid metal flow from the melting surface and retention of liquid metal on the solid substrate, with subsequent thermal interaction. Appropriate models describe the oxidation kinetics of the metal surface over the range of conditions from ambient temperature to the metal melting temperature and allow the prediction of metal ignition due to a variety of ignition modes, i.e., radiation, mechanical friction and exposure to high ambient temperatures.

Details of the program and of the analytical model are described in Reference 6. The analytical model is incomplete at this time, but development is continuing under an extension of the Reference 5 contract.

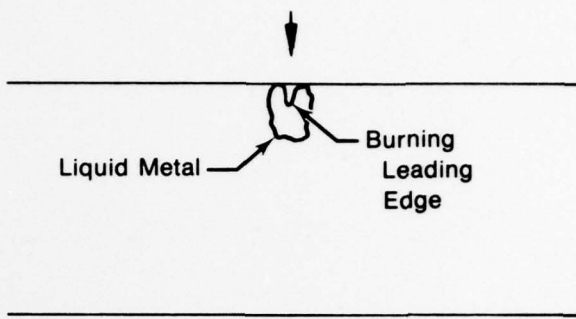
The model has been used to simulate one of the tests in the current program, namely run No. 2-1, for a total simulated real time of 0.35 second after ignition. The results are presented by the computerized model as a graphic display of the specimen, showing the progression of burning and flow of liquid metal over the surface. Figure 16 shows a comparison of the simulation with actual test results taken from the high speed film as the burning progresses. The analyzed specimen is the same geometry as that burned in run No. 2-1. The coordinates X and Y are in the flow-wise and spanwise directions, with X=0 representing the initial leading edge. The circles are the leading edge at the simulated time, indicating the extent of burning, and the small crosses represent the extent of liquid metal flow on the surface.

Comparison of the predicted and measured burning rates in the flow direction are shown in figure 17. Predicted burning rate appears to be in good agreement with measured data for this case. However, comparison of graphic simulation with movies taken during the test (Figure 16) indicates excessive lateral spreading of the predicted combustion zone. This is one of the areas of the model requiring further development under the continuing program.

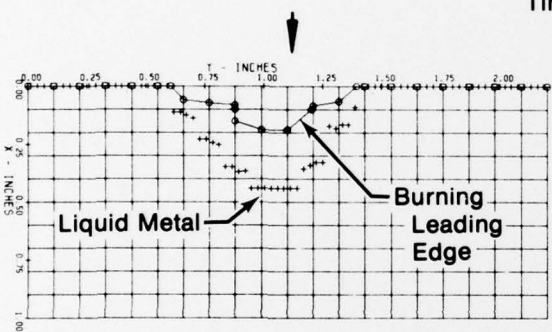
**Analytical Simulation**



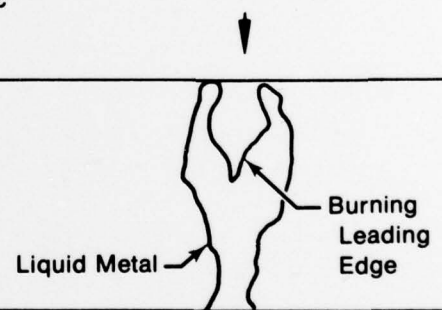
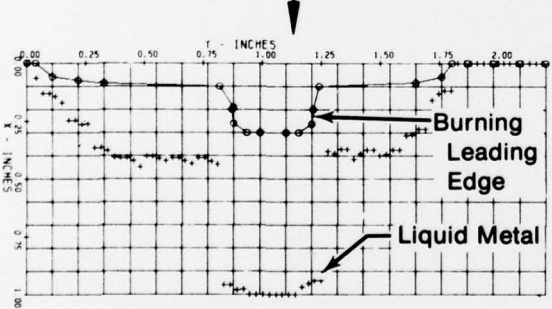
**Test Run Results**



Time = 0.05 sec



Time = 0.15 sec



↓ = Direction of Air Flow  
Specimen Number 2-1

Temperature = 804°F  
Pressure = 71 psia  
Velocity = 789 ft/sec

FD 124495

*Figure 16. Comparison of Analytical Simulation With Actual Test Results*

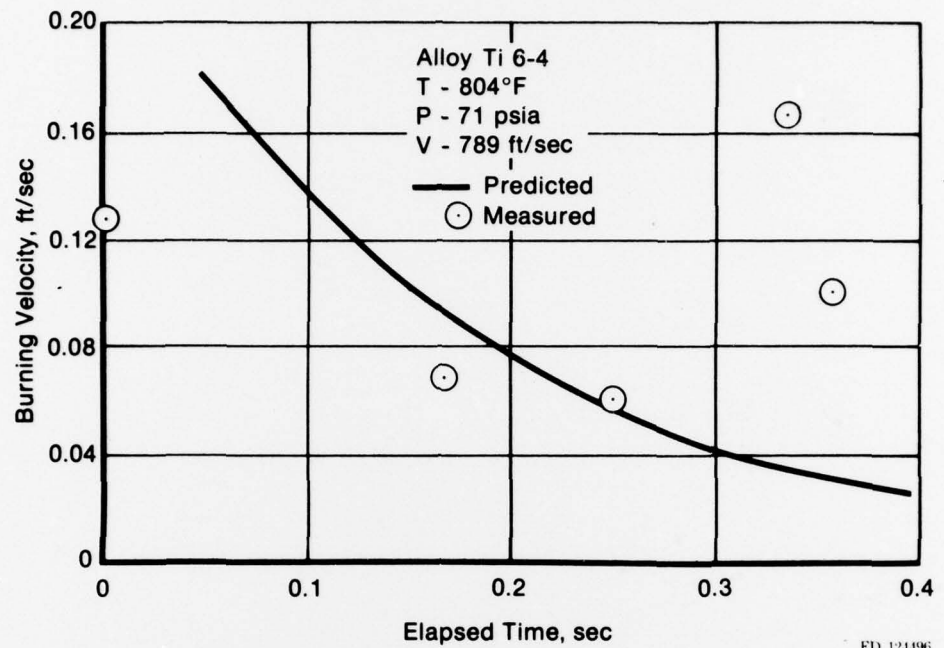


*Figure 17. Comparison of Flowwise Burning Rate for Run No. 2-1 Predicted by Model and as Measured*

## **SECTION V**

### **CONCLUSIONS**

Based upon the experimental results obtained during this program, the following conclusions were reached relative to the influence of various factors on the ignition and sustained combustion of coated and uncoated titanium alloy specimens.

#### **ALLOY EFFECTS**

1. Only slight differences could be observed in the combustion characteristics of Ti 8-1-1, Ti 6-4, Ti 6-2-4-2, Ti 6-2-4-6, Ti 6-6-2 and Ti 8 Mn.
2. Alloys Ti 13-11-3, Ti<sub>3</sub>Al and Ti 13Cu were more resistant to sustained combustion than the other alloys evaluated.

#### **COATING EFFECT**

1. The chromium-molybdenum coating increased the resistance of the titanium alloy to ignition and, if ignited, it decreased the severity of burning. These effects could be attributed to the following reasons:
  - Less energy from the burning molten metal was coupled back into the titanium alloy.
  - Low melting-temperature surface alloys were formed.
  - Molten metal flow across the specimen surface did not adhere to or wet the coated surface as well as the uncoated surface.
2. The IVD aluminum coating significantly improved the resistance of Ti 8-1-1 alloy to ignition. This effect can be explained by an increased surface thermal conductivity, thereby reducing local temperatures, and the formation of low melting temperature alloys on the specimen surface.

#### **GEOMETRY EFFECTS**

Variations in specimen thickness, within the range experienced, did not prevent ignition but the data did indicate that ignition time increased with increased thickness. Similarly, increased specimen thickness increased the chordwise burn time (after ignition). In addition, strong evidence indicated that the burn severity also increased with an increase in specimen thickness.

#### **ENVIRONMENTAL EFFECTS**

1. Sufficient energy was supplied to the test specimens to effect ignition under the two environmental test conditions selected.
2. The environmental conditions of 427°C (800°F), 0.48 MPa (70 psia) and 213 m/sec (700 ft/sec) airstream velocity was more severe than 240°C (400°F), 0.62 MPa (90 psia) and 122 m/sec (400 ft/sec) airstream velocity as they related to the extent of titanium fire propagation. Ignition was more difficult at the higher temperature and velocity conditions.

### **ANALYTICAL MODEL SUBSTANTIATION**

Predicted burning rate in the airflow direction appears to be in good agreement with the measured test results for run 2-1. However, comparison of the graphic simulation with high speed motion picture frames indicates excessive lateral spreading of the predicted combustion zone which will require further development.

## **SECTION VI**

### **RECOMMENDATIONS**

As a result of the experimental work performed under this program, the following recommendations are submitted to guide future work in the area of titanium alloy ignition and combustion:

1. Testing should employ constant cross section specimens fabricated to close thickness tolerances.
2. Separate single-alloy testing should be performed to investigate the relationship between specimen thickness and combustion characteristics.
3. Alloys Ti 13-11-3, Ti<sub>3</sub>Al and Ti13Cu should be tested at more severe conditions to complete combustability evaluation.
4. Computer model prediction of experimental results should be repeated on the tested alloys when the completed model is available.

## **REFERENCES**

1. Manty, B. A. and H. R. Liss, "Wear Resistant Coatings for Titanium Alloys," Naval Air Systems Command Report Number N00019-76-C-0342; March 1977.
2. Metal Finishing Guidebook Directory, 42nd Edition, 1974, pg. 350, Metals and Plastics Publication, Hackensack, New Jersey 07601.
3. Grosse, A. V. and J. B. Conway, "Combustion of Metals in Oxygen," Industrial and Engineering Chemistry, Vol. 50, No. 4, April 1958, pp. 663-72.
4. Harrison, P. L. and A. D. Yoffe, "The Burning of Metals," Procedures of the Royal Society A. Vol. 261 Plate 3, pp. 357-370.
5. "Titanium Combustion Research," Contract F33615-76-C-5041.
6. M. R. Glickstein, B. A. Manty, S. R. Lyon, and C. W. Elrod, "Ignition and Self-Sustained Combustion of Titanium Alloys," Third DoD Conference on Laser Effects, Vulnerability and Countermeasures, July 19-22, 1977, Naval Training Center, San Diego, California (Published by DRIA Center, ERIM, P. O. Box 8618, Ann Arbor, Michigan 48107).